

## A GCM study of effects of radiative forcing of sulfate aerosol on large scale circulation and rainfall in East Asia during boreal spring

Maeng-Ki Kim,<sup>1</sup> William K. M. Lau,<sup>2</sup> Kyu-Myong Kim,<sup>3</sup> and Woo-Seop Lee<sup>1</sup>

Received 20 August 2007; revised 11 October 2007; accepted 5 November 2007; published 18 December 2007.

[1] The effect of sulfate aerosol radiative forcing on spring rainfall in East Asia are studied based on numerical simulations with the NASA finite-volume General Circulation Model (fvGCM) forced with monthly varying three-dimensional aerosol distribution from the Goddard Ozone Chemistry Aerosol Radiation and Transport model (GOCART). Result shows that radiative forcing of sulfate aerosol leads to cooling of the land surface and reduction in rainfall over central East Asia. The maximum reduction in precipitation is shifted northward relative to the maximum aerosol loading region as a result of dynamical feedback. The anomalous thermal gradient by aerosol cooling near the land surface, reduces the baroclinicity of the atmosphere, leading to a deceleration of the upper level westerly flow. The westerly deceleration induces, through ageostrophic wind adjustment, anomalous meridional secondary circulation at the entrance region of the East Asian jetstream, with strong sinking motion and suppressed precipitation near 30°N, coupled to weak rising motion and moderately enhanced precipitation over southern China and the South China Sea. These results suggest that the radiative forcing of aerosol through induced dynamical feedback with the atmospheric water cycle, may be a causal factor in the observed spring precipitation trend over East Asia. **Citation:** Kim, M.-K., W. K. M. Lau, K.-M. Kim, and W.-S. Lee (2007), A GCM study of effects of radiative forcing of sulfate aerosol on large scale circulation and rainfall in East Asia during boreal spring, *Geophys. Res. Lett.*, *34*, L24701, doi:10.1029/2007GL031683.

### 1. Introduction

[2] In East Asia, spring rainfall supplies fresh water for the early growing season and is essential for agriculture, water resources management, and flash flood control. Spring rainfall also regulates soil moisture, modulates temperature difference between continent and ocean and influences the subsequent evolution of the Asian summer monsoon [Meehl, 1994; Yang and Lau, 1998; Zhu *et al.*, 2007]. Previous studies have shown a significant long-term trend in spring precipitation over East Asia and South Korea [Yang and Lau, 2004; Xin *et al.*, 2006; Kim *et al.*, 2005]. This long-term trend pattern for the past 45 years (1954–1998) is reproduced in Figure 1, using station monthly

rainfall data from China, showing the continuous belt of diminished rainfall in central China, along the Yangtze River, and enhanced rainfall along the southeastern coast of China. Previous studies [Xin *et al.*, 2006; Yang and Lau, 2004] have suggested that remote forcing from interdecadal variations of sea surface temperature, and/or global warming may have been responsible for the spring rainfall trend. However, atmospheric general circulation model experiments with prescribed long-term sea surface temperature anomalies and coupled ocean-atmosphere models have generally been unsuccessful in reproducing this pattern, especially with respect to the rainfall reduction over central China. This raises the possibility that important local forcing may be needed to account for the observed.

[3] Atmospheric loading of aerosols associated with industrialization and urbanization in Asian countries tends to build up in the spring before the monsoon rainy season. Such a build-up may have led to a long-term direct aerosol radiative forcing, resulting in changes in the regional water cycle [Ramanathan *et al.*, 2001]. Over central China, sulfate aerosols are known to be the major sources of emissions from major industrial cities along the Yangtze River [Tu *et al.*, 2005]. Through strong scattering of solar radiation, sulfate aerosols reduce the amount of shortwave radiation reaching the earth's surface causing cooling of the surface – the so-called “solar dimming” (SDM) effect [Ramanathan *et al.*, 2005]. Because of the heterogeneous distribution of emission sources over the continent, aerosol induced SDM effects have large spatial gradient. As a result, SDM may alter the thermal heating gradient over the East Asian continent, which in turn modulates the pressure gradient, the large-scale atmospheric circulation and rainfall. In this paper, we investigate the radiative effect of sulfate aerosols and induced dynamical feedback by the atmospheric water cycle in modulating spring precipitation over East Asia. The term “dynamical feedback” used in this study is to refer the effect from atmospheric feedback when the aerosol radiative forcings are imposed.

### 2. Model Experiments

[4] Numerical experiments are conducted using the NASA finite volume General Circulation Model (fvGCM). The radiative transfer model is described by Chou *et al.* [1998], Chou and Suarez [1999], Chou *et al.* [2001], and Chou *et al.* [2002]. The extinction coefficient, single scattering albedo, and asymmetric factor for each of the five aerosol types (sulfate, dust, black carbon, organic carbon and sea salt) are determined as a function of relative humidity and wavelength of 11 broad bands, based on Mie theory. The fvGCM uses the McRAS (Microphysics of clouds with the Relaxed Arakawa-Schubert Scheme)

<sup>1</sup>Department of Atmospheric Science, Kongju National University, Gongju, Korea.

<sup>2</sup>Laboratory for Atmospheres, NASA Goddard Space Flight Center, Greenbelt, Maryland, USA.

<sup>3</sup>Goddard Earth Sciences and Technological Center, University of Maryland Baltimore County, Baltimore, Maryland, USA.

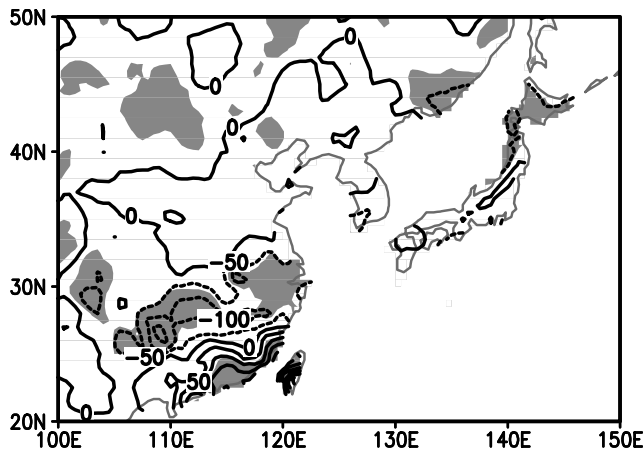


**Figure 1.** Spatial pattern of observed linear trend of spring precipitation for 45 years from 1954 to 1998. Contour interval is 50mm/45yr and significance level of 5% is shaded.

moist convection parameterization scheme [Sud and Walker, 1999], which was developed with the aim of representing moist processes, microphysics of clouds, and cloud-radiation interactions. Aerosol optical thicknesses (AOT) of each aerosol types are prescribed with three-dimensional monthly mean values for two years (2000–2001), from the Goddard Ozone Chemistry Aerosol Radiation and Transport (GOCART) model [Chin *et al.*, 2003]. Experiments with various combinations of aerosols have been carried out [see Lau *et al.*, 2006]. Only experiments with sulfate aerosols are described in this work. This work is focused on the response and dynamical feedback of the atmospheric water cycle induced by direct effects of sulfate aerosol only. Indirect effects of aerosols will be included in future work.

[5] We performed two 10-year long baseline model experiments, with sulfate aerosol (SA) and with no aerosols (NA). The sea surface temperature (SST) is prescribed, using the weekly SST from September 1986 to December 1996, interpolated to daily values. All greenhouse gases and biosphere forcing are kept the same in both simulations. The fvGCM used in this study has a horizontal resolution of 2 by 2.5 degrees and 55 vertical levels. Since all external forcings are identically prescribed between SA and NA and the aerosol forcing is repeated each year, the 10-year integration provide sufficient sampling to evaluate the mean signal with respect to the variability due to internal dynamics. Hence sulfate aerosol forcing is, by design, the root cause of any significant differences between the two experiments.

### 3. Results

#### 3.1. Climatological Features

[6] Figures 2a and 2b show climatological (10-year), March–April–May (MAM) mean precipitation of observation and model during spring in East Asia. Although there are notable differences, the model simulates reasonably well the extent and the orientation of the spring rain band from southern China to Japan. The model appears to overestimate the amount of precipitation over central and southern China. Figure 2c shows the observed MAM climatological mean 200 hPa divergence field (contour) and zonal wind (shaded) fields. An upper level divergence (positive contour) center is found around the Yangtze River south of the zonal wind maximum, while an upper level convergence (negative contour) center is found over northern China, north of the zonal wind maximum. The upper level divergence center is approximately collocated with the precipitation center (Figure 2a) indicating the presence of a secondary circulation near the jet entrance region, with

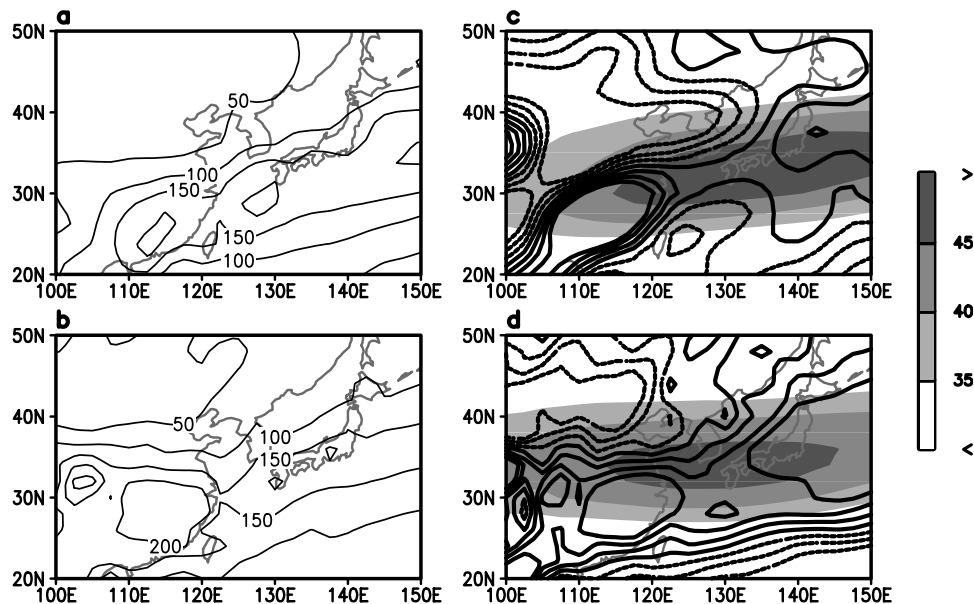


**Figure 2.** Spatial distribution of climatological precipitation (mm/month) by (a) Global Precipitation Climatology Project (GPCP) observation (1979 to 2006) and (b) model simulation (10 years), (c) zonal wind (shaded) and divergence field (contour) at 200hPa for Observation (NCEP/NCAR, 1979 to 1998), and (d) model simulation (10 years) during spring. Contour intervals for Figures 2a, 2b, 2c, and 2d are 50 mm/month, 50 mm/month,  $0.5 \times 10^{-6} \text{ S}^{-1}$ ,  $0.5 \times 10^{-6} \text{ S}^{-1}$ , respectively.

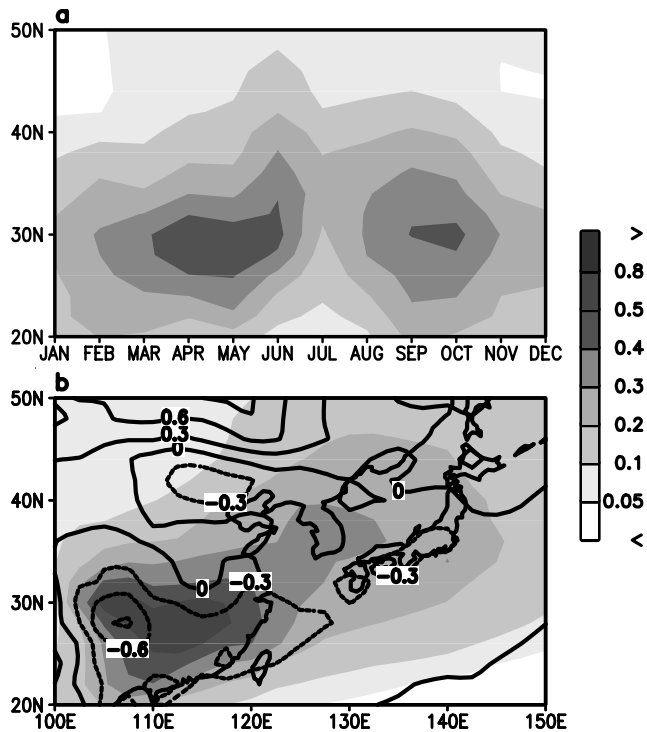


**Figure 3.** (a) Latitude-month distribution of aerosol optical thickness (AOT) of sulfate aerosol over the longitude band (110–120°E). (b) Horizontal distribution of AOT of sulfate aerosol (shaded) and surface air temperature anomaly (contour) during spring. Contour interval of surface air temperature anomaly is 0.3°C.

rising (sinking) motion south (north) of the jet core. This secondary circulation provides a poleward ageostrophic wind component ( $v_a > 0$ ), which provides the westerly acceleration ( $Du_g/Dt = f_o v_a > 0$ ) in maintaining the East Asian jetstream [Holton, 2004]. Here  $u_g$  and  $f_o$  indicate geostrophic zonal wind and Coriolis parameter, respectively. In the control run (NA experiment, Figure 2d) the divergence field and relationship with the zonal wind and precipitation are overall well simulated, although differs from observations in detailed regional features. These results indicate that despite the coarse resolution of the fvGCM, the large-scale circulation and rainfall features are reasonably well simulated by the model, thus reassuring that the fvGCM is a useful tool for the purpose of this study.

[7] To better understand the dynamical response to sulfate aerosol forcing, the distribution of sulfate AOT used by the model as forcing function need to be described first. As shown in the latitude-time section of sulfate AOT over the East Asian sector (110–120°E), there is a distinct semi-annual seasonal cycle in sulfate AOT over central China, indicating maximum loading in spring and fall. The largest build-up begins in March, peaks in May and diminishes in June through July due to washout by the monsoon rain. The reduction in AOT in November through January is likely due to the advection by the prevailing northerly low-level wind of the winter monsoon [Lau and Chang, 1992], which transport the sulfate aerosols to regions further south. Here, we focus only on the build-up phase during MAM. The MAM sulfate AOT (Figure 3b) shows a maximum over the

China south of the Yangtze River reflecting the source regions of major industrial cities [Tu et al., 2005]. The elongated spatial pattern that extends from China to Korea reflects aerosol transport by the western Pacific subtropical high, a persistent circulation in the northern hemisphere during the boreal spring and summer [Lau et al., 2000]. Note that the center of upper level divergence at 200 hPa shown in Figure 2d appears over the northeastern part of maximum sulfate AOT (Figure 3b).

### 3.2. Aerosol Direct Forcing and Dynamical Feedback

[8] The SDM effect by sulfate aerosol is apparent from the change (SA-minus-NA) in spatial pattern of surface air temperature (Figure 3b). The large surface cooling roughly coincides with the region of maximum sulfate AOT, with magnitudes of 0.3–0.6. The surface cooling is largely a local direct effect of sulfate AOT as indicated by the nearly linear decrease in surface air temperature as a function of AOT (see Table 1) Note that the center of cooling is slightly offset to the west from the center of maximum AOT, and that away from the AOT source region, alternate surface warming and cooling regions are found in the meridional direction, over northern China and northeastern Mongolia up to 50°N. These are due to dynamical effects induced by the aerosol forcing, as discussed next.

[9] Figure 4a shows the precipitation anomaly induced by aerosol forcing during the boreal spring. Here, we notice that the significant maximum reduction of spring precipitation is shifted north-eastward relative to the position of maximum sulfate AOT. The precipitation pattern is similar to that of the upper level divergence anomaly (Figure 4b), indicating that the rainfall deficit for central China is strongly tied to upper level convergence (negative contours) associated with large-scale sinking motion. Therefore, although initial cooling is initiative by the reflection of solar radiation by sulfate aerosol and anomalous downward motion at low level may have initially occurred at the maximum AOT region, the maximum reduction of precipitation occurs north of the maximum AOT zone, in the storm track region, which controls springtime rainfall over East Asia.

[10] In the latitude-height distribution of sulfate AOT averaged over the 110–120°E longitude sector (not shown), maximum loading of sulfate aerosol is found at low levels (below 800 hPa) south of 30°N, with the axis of maximum loading tilted northward with increasing height. The pronounced cooling of the lower troposphere occurs south of 30°N is consistent with maximum AOT (Figures 4c and 3b). However, stronger atmospheric cooling appears at the upper troposphere north of 30°N. Because there is almost no sulfate aerosol in the upper troposphere, this cooling cannot be due to aerosol direct radiative effect. Rather, Figure 4d

**Table 1.** Estimates of Surface Air Temperature Anomalies Induced by the Local Effect of Sulfate Aerosols in East Asia, 10–40°N, 110–130°E

AOT of Sulfate	dT
$0.2 \leq \text{AOT} < 0.3$	–0.08
$0.3 \leq \text{AOT} < 0.4$	–0.18
$0.4 \leq \text{AOT} < 0.5$	–0.39
$0.5 \leq \text{AOT}$	–0.50

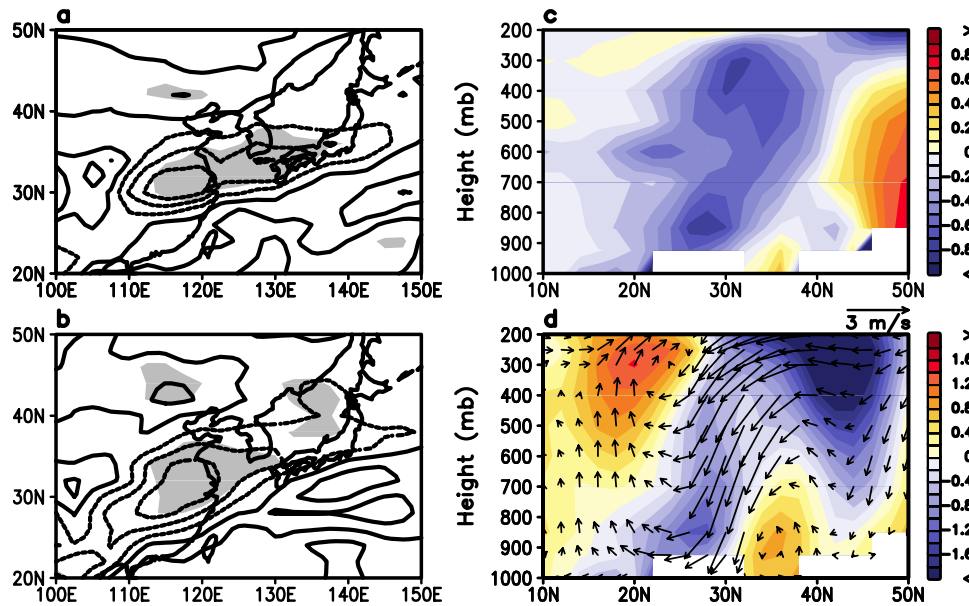


**Figure 4.** Spatial distributions of (a) precipitation anomaly and (b) upper level divergence anomaly at 200hPa. Latitude-height distribution of (c) temperature and (d) zonal wind (shading), meridional circulation anomalies (vector) averaged over the 110–120°E longitude sector induced by direct radiative forcing of sulfate aerosol during spring. Contour intervals for Figures 4a and 4b are 0.5mm/day and  $0.5 \times 10^{-6} \text{ S}^{-1}$ , respectively. Negative values are indicated by dashed lines in Figures 4a and 4b. Significance levels of 5% are shaded in Figures 4a and 4b. Units of pressure velocity and meridional wind are  $-10^{-4} \text{ hPa s}^{-1}$  and  $\text{ms}^{-1}$ , respectively.

shows that the cooling is associated with sinking motion as a part of an anomalous meridional circulation accompanying the deceleration of the upper level jetstream at the jet entrance region, as indicated by the strong negative upper level zonal wind anomaly at 40–50°N. The downward motion anomaly around 30° N is located below the upper level convergence anomaly, as shown in Figure 4b, and is associated with a negative condensation heating anomaly (not shown), which is responsible for the strong cooling of the atmospheric column.

[11] Indeed, Figure 4d shows two secondary circulation anomalies; a northern branch induced by the jet stream deceleration at 40–50°N, with sinking motion around 30°N, and a southern branch consist of sinking motion at 30°N, coupled with rising motion between 15–20°N. These anomalous secondary circulations are consistent with the anomalous divergence field at 200 hPa in Figure 4b and the precipitation anomaly in Figure 4a. The northern branch is due to the strong westerly deceleration ( $Du_g/Dt < 0$ ), i.e., a weaker jet stream, requires an equatorward ageostrophic wind component ( $v_a < 0$ ). The upper level jet deceleration stems from the reduced surface baroclinicity, i.e., warmer surface air to the south relative to the north, initially induced by sulfate AOT. The rising motion associated with the second branch is due to the forced ascent by the upper level convergence associated with the sinking air at 30°N. The rising air is sustained by increased condensation heating associated with increased rainfall over southern China and the South China Sea.

#### 4. Summary and Conclusions

[12] In this study, we find that radiative forcing by sulfate aerosol can modulate the upper level jet stream and asso-

ciated secondary circulation at an entrance of the jet core in East Asia, during the boreal spring. Sulfate aerosol initially induces surface cooling through the solar dimming effect over regions of large AOT, resulting in a reduced north-south thermal gradient. The reduced baroclinicity leads to reduced westerly wind shear through the thermal wind relationship, and a deceleration of the East Asian jetstream. The deceleration causes ageostrophic meridional winds which sets up secondary meridional circulations associated with strong upper level convergence near 30°N, south of the region of maximum westerly deceleration. It is demonstrated that a decrease of spring precipitation over Central China is induced by the upper level convergence and anomalous downward motion near 30°N, while an increase of spring precipitation over South China is caused by anomalous upward motion south of the region of upper level convergence.

[13] We note that the changes in precipitation induced by aerosol direct forcing bear some resemblance to the observed trend in Figure 1, especially with respect to the reduction of precipitation over central China. This suggests that intensity and sign of the precipitation anomaly over central China may be related to changes in jetstream dynamics induced by sulfate aerosol forcing. However, while the enhanced precipitation over southern China and the South China Sea has the correct sign, its magnitude is not well simulated. Clearly, aerosol forcing is not the only factor affecting the spring rainfall trend over East Asia. It is possible that remote forcing from sea surface temperature in the Pacific and Indian Ocean, and from interdecadal variations of large-scale circulation modes such as the North Atlantic Oscillation, or the El Nino Southern Oscillation may further modulate the rainfall distribution caused by the direct effect of aerosol forcing. Hence the dynamical feedback effect induced by sulfate aerosol radiative forcing is

only the first step in unraveling the complex causes of the long-term spring rainfall trend over East Asia. In addition, aerosol-cloud microphysics effects (indirect effects) and the land-use changes [Ho *et al.*, 2003] may also contribute to the observed trend. Further work is needed to study the interaction of the aerosol forcing (radiative and microphysics) with other dynamical remote forcing mechanisms to further understand the physical mechanisms for spring precipitation trend over East Asia.

[14] **Acknowledgments.** This work was funded by a grant (CATER 2006-4102) from the Korea Meteorological Administration Research and Development Program of the Republic of Korea. This work is partially supported by the Interdisciplinary Investigation Program of the Earth Science Division, NASA Headquarters. We thank the reviewers for helpful comments and suggestions that have much improved this paper.

## References

- Chin, M., P. Ginoux, R. Lucchesi, B. Huebert, R. Weber, T. Anderson, S. Masonis, B. Blomquist, A. Bandy, and D. Thornton (2003), A global aerosol model forecast for the ACE-Asia field experiment, *J. Geophys. Res.*, *108*(D23), 8654, doi:10.1029/2003JD003642.
- Chou, M.-D., and M. Suarez (1999), A solar radiation parameterization for atmospheric studies, *Tech. Memo. NASA/TM-1999-104606*, vol. 15, 40 pp., NASA Goddard Space Flight Cent., Greenbelt, MD.
- Chou, M.-D., M. Suarez, C.-H. Ho, M. M.-H. Yan, and K.-T. Lee (1998), Parameterizations of cloud overlapping and shortwave single-scattering properties for use in general circulation model and cloud ensemble models, *J. Clim.*, *11*, 202–214.
- Chou, M.-D., M. Suarez, X.-Z. Liang, and M.M.-H. Yan (2001), A thermal infrared radiation parameterization for atmospheric studies, *Tech. Memo. NASA/TM-2001-104606*, vol. 19, 56 pp., NASA Goddard Space Flight Cent., Greenbelt, Md.
- Chou, M.-D., K.-T. Lee, and P. Yang (2002), Parameterization of shortwave cloud optical properties for a mixture of ice particle habits for use in atmospheric models, *J. Geophys. Res.*, *107*(D21), 4600, doi:10.1029/2002JD002061.
- Ho, C.-H., J.-Y. Lee, M.-H. Ahn, and H.-S. Lee (2003), A sudden change in summer rainfall characteristics in Korea during the late 1970s, *Int. J. Climatol.*, *23*, 117–128.
- Holton, J. R. (2004), *An Introduction to Dynamic Meteorology*, 4th ed., 347 pp., Elsevier Acad., San Diego, Calif.
- Kim, S., C.-K. Park, and M.-K. Kim (2005), The regime shift of the Northern Hemispheric circulation responsible for the spring drought in Korea, *J. Korean Meteorol. Soc.*, *41*, 571–585.
- Lau, K.-M., and F. C. Chang (1992), Tropical oscillations and their predictions in the NMC operational forecast model, *J. Clim.*, *5*, 1365–1378.
- Lau, K.-M., K.-M. Kim, and S. Yang (2000), Dynamic and boundary forcing characteristics of regional components of the Asian summer monsoon, *J. Clim.*, *13*, 2461–2482.
- Lau, K.-M., M.-K. Kim, and K.-M. Kim (2006), Asian summer monsoon anomalies induced by aerosol direct forcing: The role of the Tibetan Plateau, *Clim. Dyn.*, *26*(7–8), 855–864, doi:10.1007/s00382-006-0114-z.
- Meehl, G. A. (1994), Influence of the land surface in the Asian summer on monsoon; External conditions versus internal feedbacks, *J. Clim.*, *7*, 1033–1049.
- Ramanathan, V., P. J. Crutzen, T. Kiehl, and D. Rosenfeld (2001), Aerosols, climate and the hydrologic cycle, *Science*, *294*, 2119–2124.
- Ramanathan, V., C. Chung, D. Kim, T. Bettge, L. Buja, J. T. Kiehl, W. M. Washington, Q. Fu, D. R. Sikka, and M. Wild (2005), Atmospheric brown clouds: Impacts on South Asian climate and hydrological cycle, *Proc. Natl. Acad. Sci. U.S.A.*, *102*, 5326–5333.
- Sud, Y. C., and G. K. Walker (1999), Microphysics of clouds with the relaxed Arakawa-Schubert scheme (McRAS). Part I: Design and evaluation with GATE phase III data, *J. Atmos. Sci.*, *56*, 3196–3220.
- Tu, J., H. Wang, Z. Zhang, X. Jin, and W. Li (2005), Trends in chemical composition of precipitation in Nanjing, China, during 1992–2003, *Atmos. Res.*, *73*, 283–298.
- Xin, X., R. Yu, T. Zhou, and B. Wang (2006), Drought in late spring of south China in recent decades, *J. Clim.*, *19*, 3197–3206.
- Yang, S., and K.-M. Lau (1998), Influence of sea surface temperature and ground wetness on Asian summer monsoon, *J. Clim.*, *11*, 3230–3246.
- Yang, F., and K.-M. Lau (2004), Trend and variability of China precipitation in spring and summer: Linkage to sea surface temperatures, *Int. J. Climatol.*, *24*, 1625–1644.
- Zhu, C., T. Cavazos, and D. P. Lettenmaier (2007), Role of antecedent land surface conditions in warm season precipitation over Northwestern Mexico, *J. Clim.*, *20*, 1774–1790.

K.-M. Kim, Goddard Earth Sciences and Technological Center, University of Maryland Baltimore County, 5523 Research Park Drive, Suite 320, Baltimore, MD 21228, USA.

M.-K. Kim and W.-S. Lee, Department of Atmospheric Science, Kongju National University, 182 Shinkwan-dong, Gongju 314-701, Korea. (mkkim@kongju.ac.kr)

W. K. M. Lau, Laboratory for Atmospheres, NASA Goddard Space Flight Center, Code 613, Greenbelt, MD 20771, USA.